ChemPubSoc Europe

DOI: 10.1002/chem.201303777

CHEMISTRY
A European Journal
Full Paper

Peptides

Peptide-Based Carbohydrate Receptors

Melanie Rauschenberg, Sateesh Bandaru, Mark P. Waller, and Bart Jan Ravoo*[a]

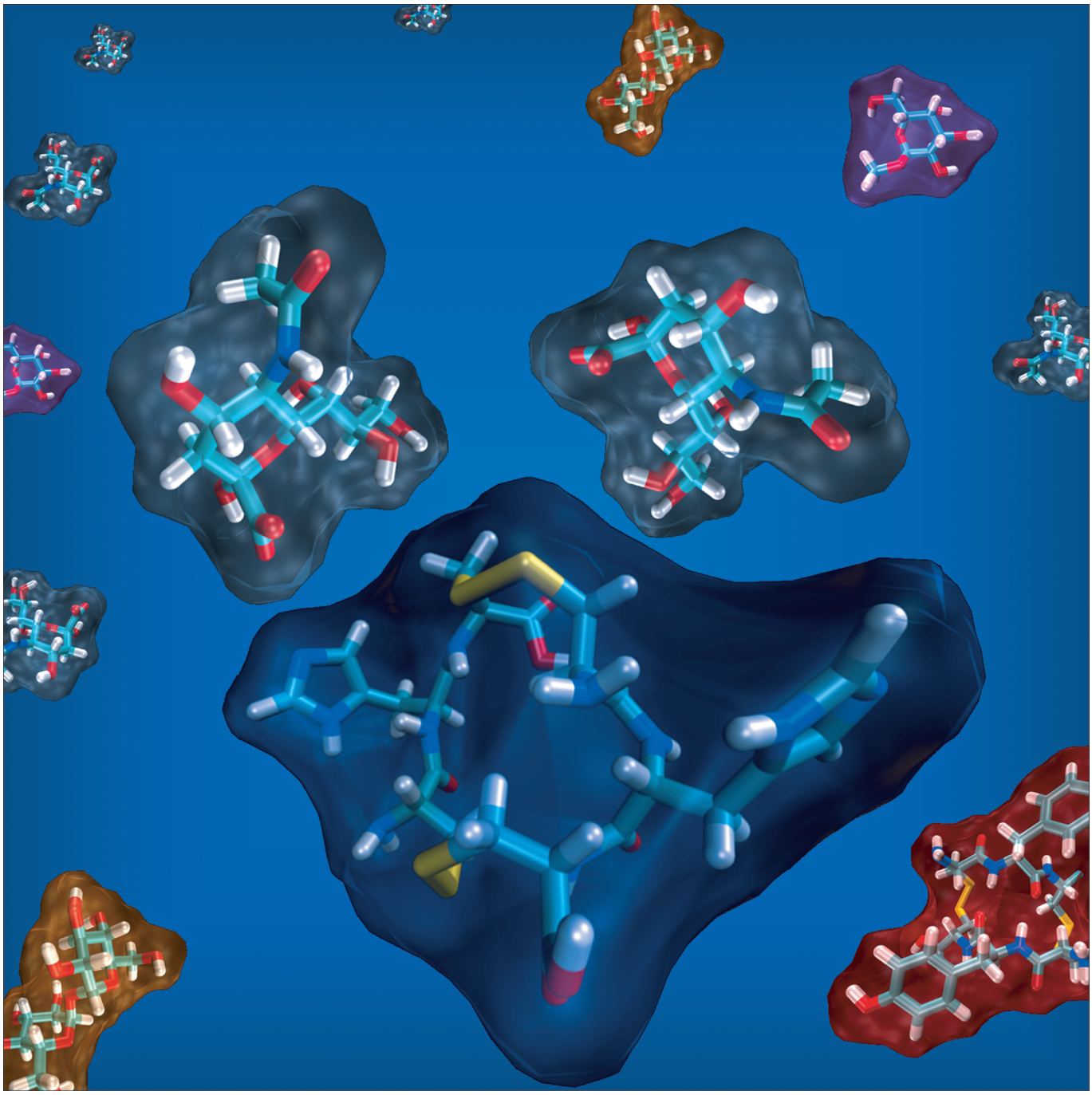

Abstract: A broad spectrum of physiological processes is mediated by highly specific noncovalent interactions of carbohydrates and proteins. In a recent communication we identified several cyclic hexapeptides in a dynamic combinatorial library that interact selectively with carbohydrates with high binding constants in water. Herein, we report a detailed investigation of the noncovalent interaction of two cyclic hexapeptides (Cys-His-Cys (which we call HisHis) and Cys-Tyr-Cys (which we call TyrTyr)) with a selection of monosaccharides and disaccharides in aqueous solution. The parallel and antiparallel isomers of HisHis or TyrTyr were synthesized separately, and their interaction with monosaccharides and disaccharides in aqueous solution was studied by isothermal titration calorimetry, NMR spectroscopic titrations, and circular dichroism spectroscopy. From these measurements, we identified particularly stable complexes ($K_a > 1000\ M^{-1}$) of the parallel isomer of HisHis with *N*-acetylneuraminic acid and with methyl-α-D-galactopyranoside as well as of both isomers of TyrTyr with trehalose. To gain further insight into the structure of the peptide–carbohydrate complexes, structure prediction was performed using quantum chemical methods. The calculations confirm the selectivity observed in the experiments and indicate the formation of multiple intermolecular hydrogen bonds in the most stable complexes.

Introduction

In biology, proteins that bind to oligosaccharides are called lectins.[1] Lectins play important roles in cell–cell recognition processes, inflammation, and infection of cells by viruses and bacteria. Lectins are an attractive yet difficult target for drug discovery and diagnostics. Carbohydrates also play a prominent role in cell–cell recognition.[2] Embedded in cell membranes in the form of glycolipids or glycoproteins, they are often found in the plasma membranes of eukaryotic cells. Oligosaccharides enhance the hydrophilic properties of the lipids and proteins and stabilize the conformation of membrane proteins. The human blood-group antigens are a well-known example of specific protein–carbohydrate interaction at the cell surface: the A, B, and 0 antigens are closely related oligosaccharides that are linked to lipids, and the ability of antibodies to differentiate between these glycolipids with only slightly different structures leads to specific immune reactions. Similarly, bacterial proteins can also selectively bind to oligosaccharides on the cell surfaces.

Owing to the complexity and stereochemical diversity of carbohydrates, the identification of "synthetic lectins" poses a phenomenal challenge to supramolecular chemists.[3] Binding of lectins to carbohydrates is mediated by hydrogen bonding, CH–π interactions, and/or metal-ion complexation. The large number of hydroxyl groups on the carbohydrate is similar to the surrounding biological solvent (i.e., water), which is therefore the main competitor for the binding site. To bind, any given carbohydrate receptor must be able to discriminate between water and the carbohydrate so that the latter is preferentially bound. The discrimination between substrate and water is far from trivial, since carbohydrates are complex and "camouflaged" by hydroxyl groups.[3] Furthermore, the differences between individual carbohydrates are very small because they all posses a similar size and similar functional groups but only differ in their stereochemistry. Recent papers on synthetic lectins exploit hydrogen bonding and CH–π interactions[4] or (non-biomimetic) boronic acids[5] to obtain highly selective and potent carbohydrate receptors that are also able to operate under aqueous conditions. Artificial receptors based on 8-hydroxyquinoline were recently shown to display binding preference for glycopyranosides.[6] Another useful type of host–guest complex includes the acetylene-linked pyridine/pyridone macrocycles that bind to mannosides.[7] Arguably the most spectacular advances in the area of synthetic lectins come from Davis and co-workers, who recently synthesized a cagelike receptor that binds glucose with excellent selectivity versus other simple carbohydrates (for example, approximately 50:1 versus galactose) and sufficient affinity for glucose sensing in blood.[8]

In 2010, we described the identification of carbohydrate receptors from tripeptides using dynamic combinatorial chemistry and the thiol–disulfide exchange reaction under thermodynamic equilibrium.[9] We showed that the N- and C-terminal cysteine residues of tripeptides Cys-X-Cys form disulfide bonds with a second Cys-X-Cys tripeptide to yield exclusively cyclic hexapeptides (Scheme 1). The cyclic hexapeptides obtained from cysteine and histidine, Cys-His-Cys (which we call HisHis), and cysteine and tyrosine, Cys-Tyr-Cys (which we call TyrTyr), showed strong and selective interactions ($K_a > 1000\ M^{-1}$ in aqueous solution at neutral pH) with *N*-acetyl neuraminic acid (NANA) and trehalose (Tre), respectively.

It should be emphasized that during the thiol–disulfide exchange reaction in the dynamic combinatorial library of Cys-X-Cys peptides, two constitutional isomers (parallel and antiparallel Cys-X-Cys; see Scheme 1) were formed. In our previous work, only the affinity and selectivity of the mixture of isomers was investigated. Herein, we report the synthesis and characterization of the parallel and antiparallel isomers by using solid-phase peptide chemistry and an orthogonal protection scheme. The affinity and selectivity of each isomer for a range of carbohydrates were studied by isothermal titration calorimetry (ITC), NMR spectroscopy, and circular dichroism (CD) titrations.

[a] *Dr. M. Rauschenberg, Dr. S. Bandaru, Dr. M. P. Waller, Prof. Dr. B. J. Ravoo*
Organic Chemistry Institute
Westfälische Wilhelms-Universität Münster
Corrensstrasse 40, 48149 Münster (Germany)
E-mail: b.j.ravoo@uni-muenster.de

Supporting information for this article is available on the WWW under http://dx.doi.org/10.1002/chem.201303777.

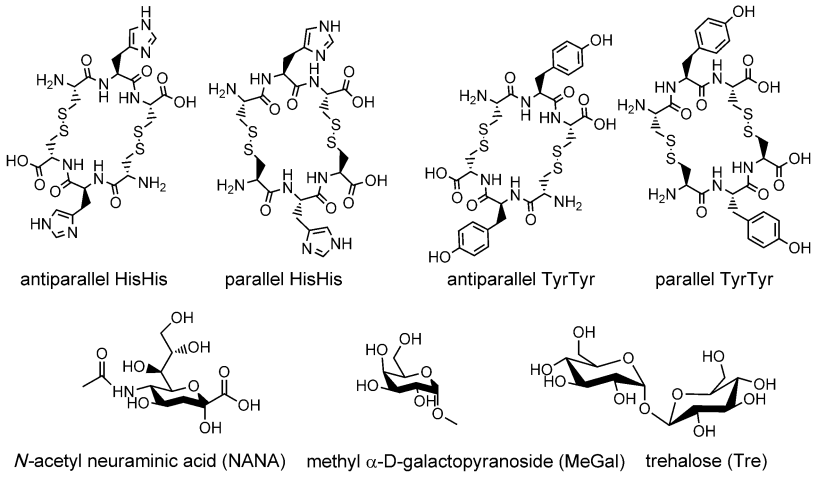

Scheme 1. Parallel and antiparallel isomers of HisHis and TyrTyr and their most important carbohydrate targets.

Furthermore, quantum chemical calculations were performed to provide structural insight into this class of peptide–carbohydrate complexes. A balanced description of the various noncovalent intermolecular interactions within the complex is the key to model realistic structures. For large systems (>100 atoms), density functional theory (DFT) has gained popularity owing to good accuracy combined with favorable scaling.[10] The deficiencies of traditional Kohn–Sham DFT toward long-range dispersion interactions[11–13] can be corrected using an additional dispersion correction term (DFT-D).[14] DFT has been extensively validated across an extremely large number of benchmark studies of weakly interacting dimers,[15–17] and therefore is a good choice for novel structure prediction of these peptide-based carbohydrate receptors.

Results and Discussion

Synthesis and characterization of cyclic peptides

Initial attempts to synthesize the parallel and antiparallel isomers of HisHis and TyrTyr on 4-methylbenzhydrylamine (MBHA) resin by using solid-phase peptide chemistry and orthogonal protection groups failed.[18] No product could be isolated after cleavage from the resin. This might be due to the formation of mixed disulfides on the beads, which leads to cross-linking of the peptide backbone. Therefore, orthogonal protection groups on the Cys residues and disulfide formation in solution were applied (see Scheme 2). The acetamidomethyl (Acm) and triphenylmethyl (trityl, Trt) groups were selected in view of the possibility of selectively cleaving the Acm group and simultaneously forming the desired disulfide bond. The Trt group is readily deprotected when cleaving the peptide of the resin. In the case of the parallel isomers of HisHis and TyrTyr, the free thiol function is used to perform the disulfide exchange reaction, which leads to the formation of the first disulfide bridge. Upon cleavage of the Acm group with iodine under acidic conditions, the second disulfide bridge was obtained in reasonable yield.[19]

In the case of the antiparallel isomers of HisHis and TyrTyr, the free thiol function was derivatized with a reactive disulfide by using dithiodipyridine to prevent formation of the undesired linear homodimer (Scheme 3).[20] Afterwards, the inverse Acm-protected tripeptide was coupled using the thiol–disulfide exchange reaction to yield the desired (inverse) linear hexapeptide. Upon cleavage of the Acm group under the same conditions as mentioned above, the antiparallel cyclic dimer was obtained in good yield.

Details of the synthesis of the parallel and antiparallel cyclic hexapeptides can be found in the Supporting Information. For the purpose of comparison, the mixture of isomers was also synthesized simply by stirring the tripeptides (Cys-His-Cys or Cys-Tyr-Cys) with two free thiol functions under basic condi-

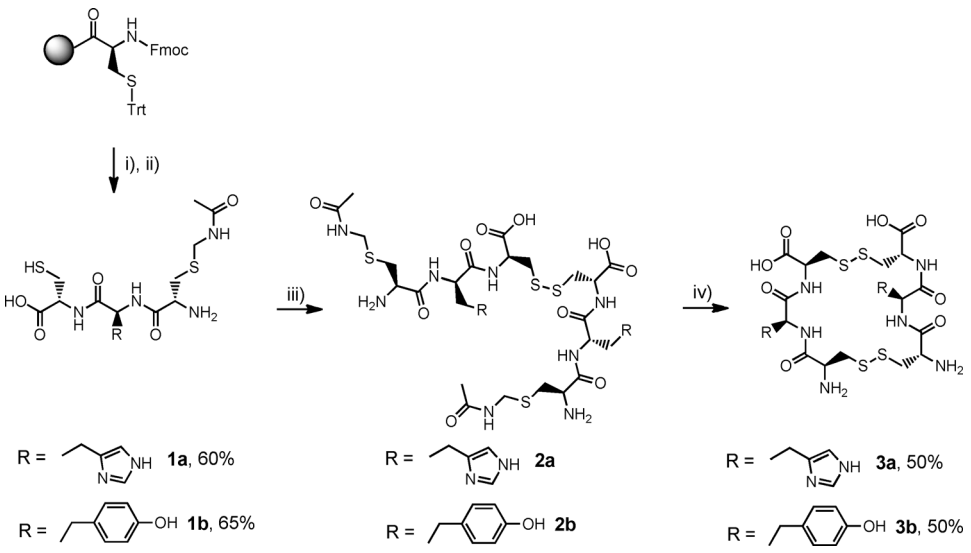

Scheme 2. Synthesis of the parallel isomers of HisHis (**3a**) and TyrTyr (**3b**): i) 20% piperidine in DMF, 20 min, RT/Fmoc-His(Trt)–OH (Fmoc = fluorenylmethyloxycarbonyl) or Fmoc-Tyr(*t*Bu)OH, *N*,*N*′-diisopropylcarbodiimide (DIPCDI), Oxyma pure, DMF, 2 h, RT/20% piperidine in DMF, 20 min, RT/Fmoc-Cys(Acm)–OH, DIPCDI, Oxyma pure, DMF, 2 h, RT; ii) 94% trifluoroacetic acid (TFA), 1% triisopropylsilane (TIS), 2.5% H_2O, and 2.5% 1,2-ethanedithiol (EDT), 6 h, RT; iii) Milli-Q, aqueous NaOH, 4 d, RT; iv) 118 mM I_2, 334 mM HCl, AcOH, 2 h, RT.

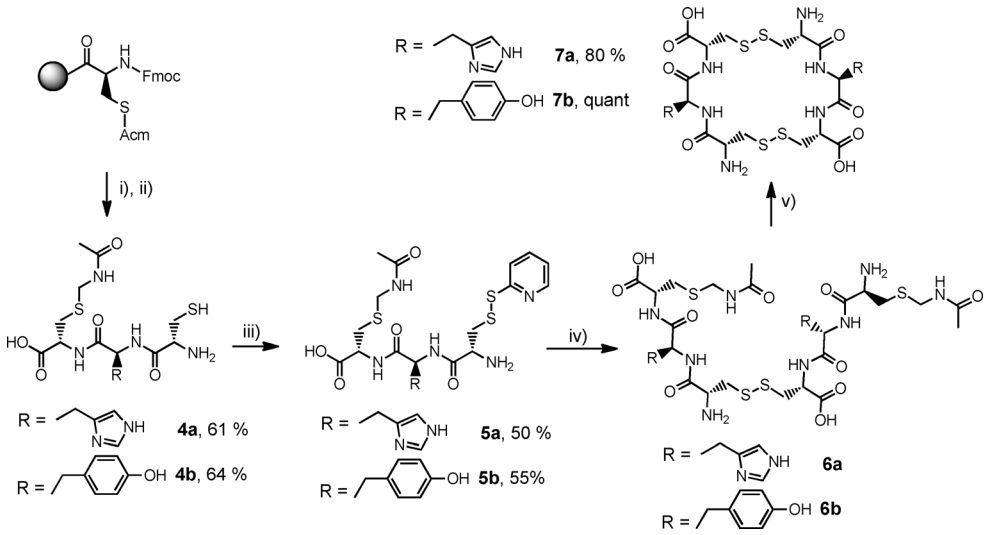

Scheme 3. Synthesis of the antiparallel isomers of HisHis (**7a**) and TyrTyr (**7b**): i) 20% piperidine in DMF, 20 min, RT/Fmoc-His(Trt)–OH or Fmoc-Tyr(*t*Bu)OH, DIPCDI, Oxyma pure, DMF, 2 h, RT/20% piperidine in DMF, 20 min, RT/Fmoc-Cys(Trt)–OH, DIPCDI, Oxyma pure, DMF, 2 h, RT; ii) 94% TFA, 1% TIS, 2.5% H_2O, and 2.5% EDT, 6 h, RT; iii) dithiodipyridine (1 equiv), 2 M HOAc/MeOH = 10:1, 24 h, RT; iv) compound **1a** or **1b**, 0.1% HOAc/10 mM NH_4OAc (pH 6.0), 24 h, RT; v) 118 mM I_2, 334 mM HCl, AcOH, 2 h, RT.

tions for 2 days. The purity of the isomers as well as the composition of the mixture was determined with HPLC by using hydrophilic interaction liquid chromatography (HILIC). The HPLC traces for both isomers of HisHis and TyrTyr as well as the mixture of isomers are shown in Figures S1 and S2 of the Supporting Information.

Isothermal titration calorimetry

The selectivity of the interaction of the HisHis and TyrTyr isomers with different carbohydrates was studied using ITC. In our previous work we had established that the mixture of HisHis isomers binds NANA in a cooperative 1:2 complex (1 molecule of HisHis binds 2 molecules of NANA) with rather strong binding constants $K_1 = 70\ M^{-1}$ and $K_2 = 7.76 \times 10^3\ M^{-1}$ at neutral pH in water.[9] From the ITC titration of parallel HisHis (**3a**) and antiparallel HisHis (**7a**) with NANA, it is evident that both isomers interact with NANA in a 1:2 complex, but a significantly stronger binding of the parallel isomer is observed (see Table 1; Figure S3 in the Supporting Information). Nevertheless, both HisHis isomers are potent cooperative receptors for the binding of two equivalents of NANA in aqueous solution. The binding constants (K_a) are higher, the binding enthalpy (ΔH) is more negative, and the binding entropy (ΔS) is more positive for the parallel HisHis than the antiparallel HisHis. These findings are in agreement with HPLC data reported previously for a dynamic combinatorial library of peptides that contain Cys-His-Cys, which displayed a higher amplification of the parallel isomer of HisHis relative to the antiparallel isomer of HisHis upon addition of NANA.[9] It can be seen in Table 1 that for each isomer of HisHis, the binding of the second molecule of NANA is considerably more favorable than the binding of the first molecule of NANA: K_2 is more than one order of magnitude larger than K_1 in each case. Binding of the second NANA is driven by a substantial increase in entropy, which likely originates from significant dehydration of both HisHis and NANA upon complexation. This clearly suggests that cooperativity is the result of receptor preorganization by the first NANA, which leads to an entropic penalty for the binding of the first NANA relative to the second NANA. The higher affinity of the parallel HisHis than the antiparallel HisHis should be a consequence of the structural difference and the relative stability of each isomer, which will be discussed on the basis of the DFT results (see below).

Table 1. Thermodynamic data for the interaction of HisHis and TyrTyr isomers (parallel, antiparallel, and a mixture of both) with selected carbohydrates measured by isothermal titration calorimetry.

Peptide	Carbohydrate	*n*	K_a [M^{-1}]	ΔG [kJ mol^{-1}]	ΔH [kJ mol^{-1}]	ΔS [J K^{-1} mol^{-1}]
mixed HisHis	NANA	1:2	$K_1 = 72.7$ $K_2 = 7.76 \times 10^3$	$\Delta G_1 = -10.6$ $\Delta G_2 = -22.2$	$\Delta H_1 = -6.27$ $\Delta H_2 = -1.54$	$\Delta S_1 = 14.6$ $\Delta S_2 = 69.4$
parallel HisHis	NANA	1:2	$K_1 = 143$ $K_2 = 5.08 \times 10^3$	$\Delta G_1 = -12.6$ $\Delta G_2 = -21.2$	$\Delta H_1 = -11.40$ $\Delta H_2 = -2.73$	$\Delta S_1 = 3.0$ $\Delta S_2 = 61.8$
antiparallel HisHis	NANA	1:2	$K_1 = 94$ $K_2 = 990$	$\Delta G_1 = -11.3$ $\Delta G_2 = -17.1$	$\Delta H_1 = -5.46$ $\Delta H_2 = -2.61$	$\Delta S_1 = 19.5$ $\Delta S_2 = 48.6$
mixed HisHis	MeGal	1:1	9.28×10^3	−10.6	−0.39	78.7
parallel HisHis	MeGal	1:1	7.96×10^3	−22.7	−0.22	75.4
antiparallel HisHis	MeGal	n.a.[a]	n.a.[a]	n.a.[a]	n.a.[a]	n.a.[a]
mixed TyrTyr	Tre	1:1	2.85×10^3	−9.7	−2.89	56.5
parallel TyrTyr	Tre	1:1	930	−16.7	−4.07	42.3
antiparallel TyrTyr	Tre	1:1	1.19×10^3	−18.1	−5.73	41.5

[a] Not applicable.

Unexpectedly, investigation of the interaction of parallel HisHis and antiparallel HisHis with methyl-α-D-galactopyranoside (MeGal) by ITC revealed a weakly endothermic but highly entropically favored binding of the parallel HisHis isomer exclusively (see Figure S4 in the Supporting Information). The raw data obtained from this titration could be readily fitted to a 1:1 model and gave a binding constant of $K_a = 5.12 \times 10^3\ M^{-1}$. In the case of antiparallel HisHis, only a very small heat of dilution was observed in the ITC measurement (see Figure S4 in the Supporting Information). Thus, in contrast to the interaction of HisHis with NANA, the interaction of HisHis with MeGal is 1:1 (not 1:2), endothermic (not exothermic), and highly selective toward the parallel isomer. Evidently, the selective interaction of the parallel isomer of HisHis with NANA can only be explained from the structure and the relative stability of the parallel and antiparallel isomers, which will be discussed on the basis of the DFT results (see below).

It should be emphasized that the monosaccharides methyl α-D-glucopyranoside (MeGlc), methyl α-D-mannopyranoside (MeMan), and methyl α-D-fucopyranoside (MeFuc) as well as the disaccharides sucrose (Suc) and trehalose (Tre) showed no significant interaction with any of the HisHis isomers (see Figure S5 in the Supporting Information). These control experiments confirm that parallel HisHis is a selective receptor for NANA and MeGal that does not bind to several very similar carbohydrates.

The selectivity of the TyrTyr isomers with different carbohydrates was also studied using ITC (see Table 1; Figure S6 in the Supporting Information). In our previous work we had established that the mixture of TyrTyr isomers binds with Tre in a 1:1 complex with a rather strong binding constant $K_a = 2.85 \times 10^3\ M^{-1}$ at neutral pH in water.[9] It was found that both isomers of TyrTyr bind with Tre with nearly the same affinity. The interaction is exothermic and entropically driven. The raw data could be readily fitted with a 1:1 model (see Figure S6 in the Supporting Information) to give the binding constants shown in Table 1. It should be noted that the quality of the ITC data was affected by the low solubility of TyrTyr in the phosphate buffer at the concentrations necessary for ITC. The observation that both isomers of TyrTyr have the same affinity for Tre is in agreement with HPLC data reported previously for a dynamic combinatorial library of peptides that contain Cys-Tyr-Cys, which displayed an equal amplification of each isomer upon addition of Tre.[9] We note that the monosaccharides NANA, MeGal, MeGlu, MeMan, and MeFuc as well as the disaccharide Suc showed no interaction with either of the TyrTyr isomers (see Figure S7 in the Supporting Information). These control experiments confirm that TyrTyr is a selective receptor for Tre relative to several very similar carbohydrates.

NMR spectroscopic titrations

The formation of hydrogen bonds in the peptide–carbohydrate complexes was studied by using ^{1}H NMR spectroscopic measurements of the parallel and antiparallel isomers of HisHis isomers as well as of the 1:1 and 1:2 complex of each HisHis isomer with NANA in 100 mM phosphate buffer at pH 7.4. Suppression of the water signal by using an excitation sculpting pulse sequence identifies NH and OH protons that are not exchanging or slowly exchanging with the aqueous solvent.[21]

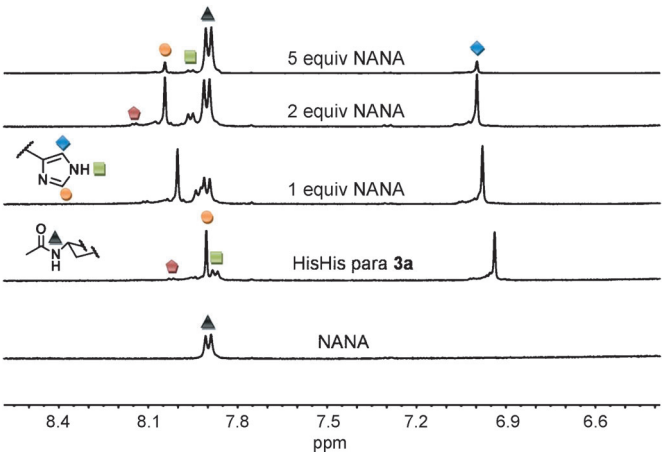

Figure 1. Aromatic region of the ^{1}H NMR spectra of parallel HisHis, NANA, and their 1:1, 1:2, and 1:5 mixtures.

The aromatic region of the NMR spectra obtained for parallel HisHis (2 mM), NANA (2 mM), their 1:1 mixture (2 mM each), their 1:2 mixture (2 mM parallel HisHis and 4 mM NANA), and their 1:5 mixture (2 mM parallel HisHis and 10 mM NANA) are shown in Figure 1. Upon addition of one equivalent of NANA to parallel HisHis, the imidazole protons are shifted downfield (Figure 1: marked by a blue diamond and orange circle are shifted by $\delta = 0.041$ and 0.10 ppm, respectively) owing to hydrogen-bond formation. This is confirmed by the simultaneous downfield shift of the imidazole NH protons (Figure 1; marked by a green square and shifted by $\delta = 0.058$ ppm). Furthermore, amide protons of the peptide backbone of HisHis (red pentagon) are also shifted downfield by $\delta = 0.086$ ppm. At the same time, the amide proton of NANA (black triangle) does not show any shift, which indicates that it is not involved in the interaction with parallel HisHis. Addition of two equivalents of NANA leads to further downfield shifts of the imidazole resonances (Figure 1: marked by a blue diamond and orange circle are shifted by $\delta = 0.018$ and 0.042 ppm, respectively), the imidazole NH protons (marked by a green square and shifted by $\delta = 0.026$ ppm), and the amide protons in the backbone (marked by a red pentagon and shifted by $\delta = 0.036$ ppm). The observed shifts are only half of what was found for the 1:1 mixture. Further addition of NANA up to five equivalents did not result in significant shifts of any proton. The NMR spectroscopic experiments indicate that binding of parallel HisHis and NANA involves the formation of hydrogen bonds by the imidazole residues of HisHis as well as the peptide backbone of HisHis. The amide group of NANA does not participate in the binding.

From ^{1}H NMR spectroscopic water suppression experiments with antiparallel HisHis (2 mM) and NANA (0–10 mM), the spectra shown in Figure 2 were obtained. In this case, the downfield shift observed for the imidazole protons (Figure 2: marked by a blue diamond and orange circle are shifted by

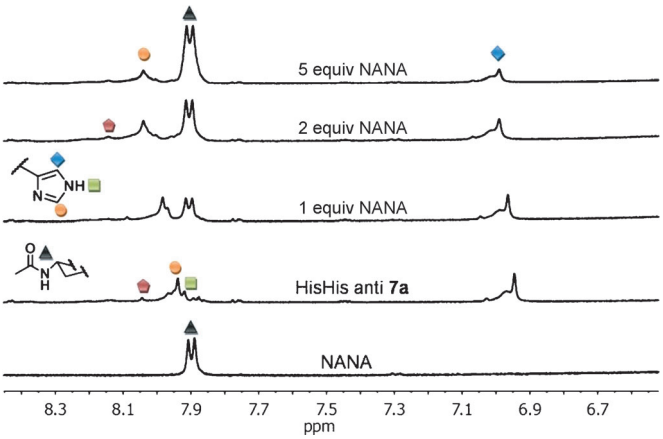

Figure 2. Aromatic region of the ^{1}H NMR spectra of antiparallel HisHis, NANA, and their 1:1, 1:2, and 1:5 mixtures.

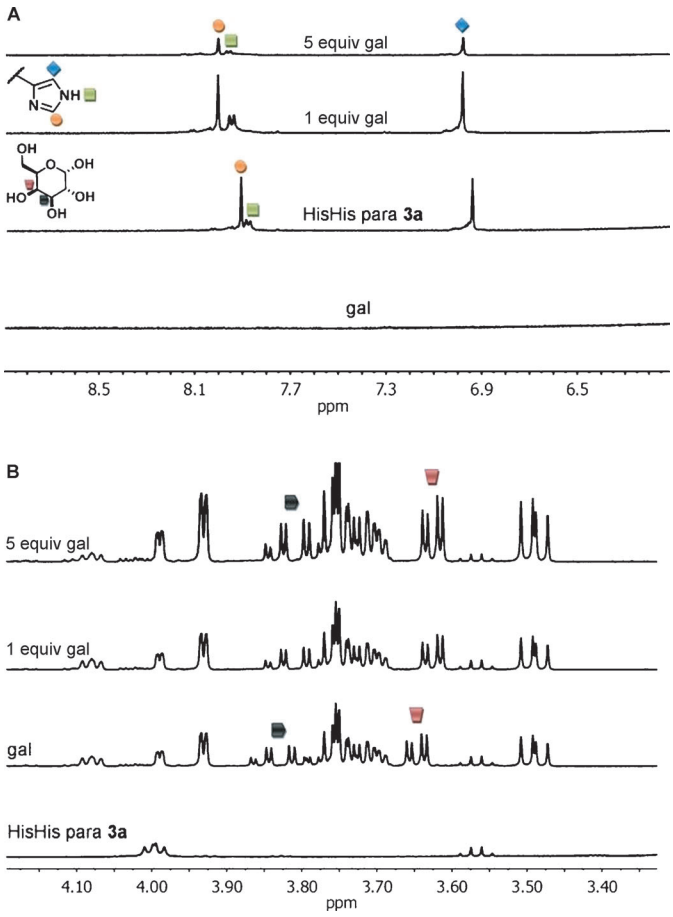

Figure 3. ^{1}H NMR spectra of A) the aromatic region and B) the carbohydrate region of parallel HisHis (**3a**), Gal, their 1:1 mixture, and their 1:5 mixture.

$\delta = 0.020$ and 0.044 ppm, respectively) and the amide protons in the peptide backbone (marked by a red pentagon and shifted by $\delta = 0.043$ ppm) in the presence of one equivalent of NANA is only half of the shift that was found for the parallel HisHis isomer. A shift of the imidazole NH protons (green square) cannot be determined owing to overlapping with the amide signal of NANA. No significant shift was detected for the amide proton of NANA (black triangle). Addition of two equivalents NANA results in further downfield shifts of the imidazole protons (Figure 2: marked by a blue diamond and orange circle are shifted by $\delta = 0.026$ and 0.057 ppm, respectively) and the amide protons in the backbone (marked by a red pentagon and shifted by $\delta = 0.058$ ppm). Relative to the parallel isomer of HisHis, for which the second equivalent of NANA resulted in smaller shifts, the shifts observed for the antiparallel isomer are slightly larger than the ones found for the 1:1 complex. When the amount of NANA was increased to five equivalents, no further shifts were detected.

^{1}H NMR spectroscopic water suppression experiments of the parallel isomer of HisHis (2 mM) and D-galactopyranose (Gal; 0–10 mM) in 100 mM phosphate buffer at pH 7.4 showed a downfield shift of the imidazole protons (Figure 3a: marked by an orange circle and blue diamond and are shifted by $\delta =$ 0.10 and 0.038 ppm, respectively) of HisHis in the presence of one equivalent of Gal, thus indicating hydrogen-bond formation. Additionally, the imidazole NH protons (Figure 3a, marked by a green square and shifted by $\delta = 0.059$ ppm) shifted downfield. In contrast, two CH protons (Figure 3b, black and red squares) of Gal are shifted upfield by $\delta = 0.025$ and 0.023 ppm, respectively, which also indicates hydrogen-bond formation of the corresponding OH functions. Thus, the NMR spectroscopic experiments indicate that binding of parallel HisHis and Gal involves the formation of hydrogen bonds by the imidazole residues of HisHis with OH groups of Gal. Addition of up to five equivalents of Gal did not result in any changes relative to the spectra when one equivalent of Gal was added. Experiments with antiparallel HisHis and Gal resulted in no significant shifts of the imidazole moieties or of the carbohydrate protons (Figure S7 in the Supporting Information), thus indicating no significant interaction, which is in good agreement with the results obtained by ITC titration.

In summary, the results obtained by ^{1}H NMR spectroscopy and ITC for the complexes of the isomers of HisHis with NANA and MeGal, respectively, are fully consistent, but the basis for the observed selectivity remains uncertain. One explanation might be the different conformations of the parallel and antiparallel HisHis isomers. Nuclear Overhauser effect (NOE) measurements of either of the isomers in the presence of NANA and Gal were inconclusive owing to the high flexibility of the receptors, which gives rise to a large number of different conformations present in the solution. In case of the TyrTyr and Tre, no significant shifts can be detected upon addition of Tre (see Figures S9 and S10 in the Supporting Information). Also in this case, NOE measurements were inconclusive owing to the large number of possible conformations present in solution.

CD measurements

The carbohydrate complexes of HisHis and TyrTyr were also investigated by CD measurements. It was found that the isomers of HisHis did not display significant changes in their CD spectrum in the presence of NANA so that no meaningful informa-

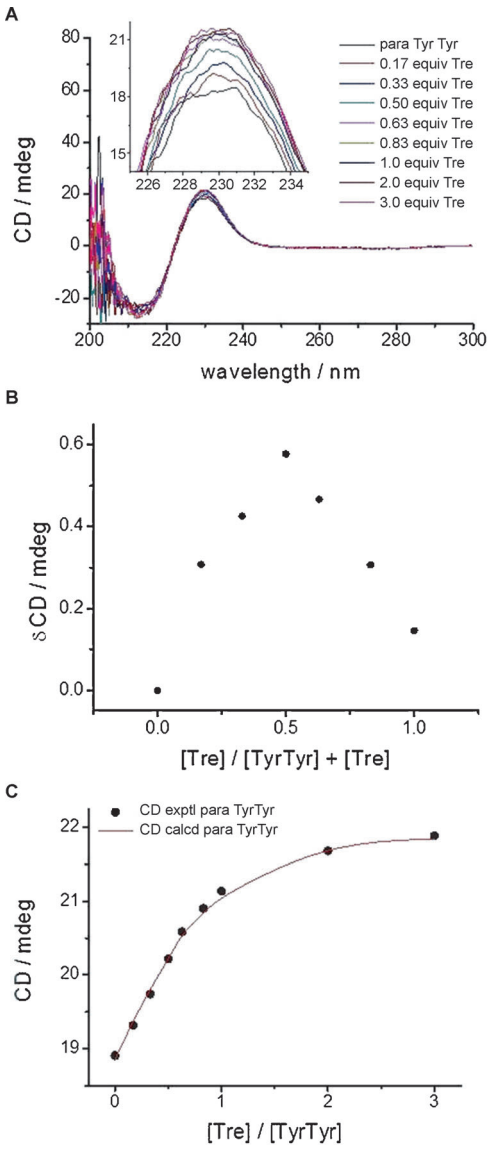

Figure 4. A) CD spectra upon titration of 80 mM trehalose to a 2 mM solution of the parallel isomer of TyrTyr in phosphate buffer (100 mM, pH 7.4). B) Job plot of the titration data. C) Fit of the titration data.

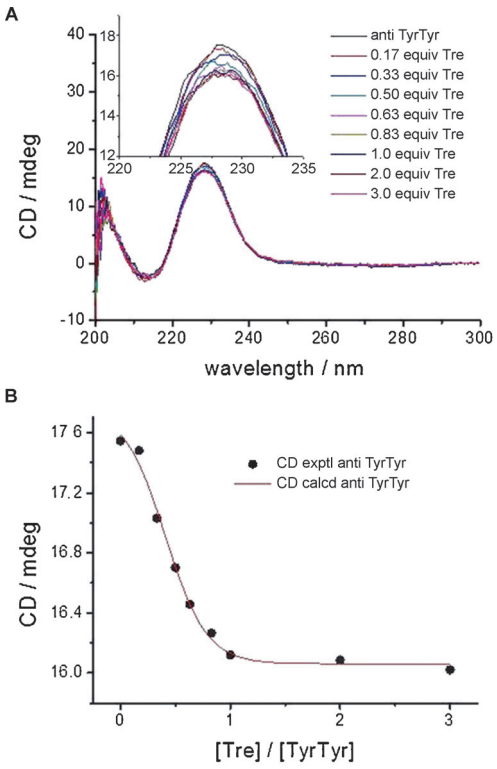

Figure 5. A) CD spectra upon titration of 80 mM trehalose into a 2 mM solution of the antiparallel isomer of TyrTyr in phosphate buffer (100 mM, pH 7.4). B) Fit of the titration data.

tion could be obtained for this complex by using this method. However, the tyrosine moieties in TyrTyr show significant UV absorption and Cotton bands at higher wavelength. The different conformations of the parallel and antiparallel isomers are evident from the different CD signals for each isomer (see Figures 4a and 5a). The CD effect observed for the tyrosine moieties upon addition of Tre is rather small but the disulfide bonds show a significant CD effect at 230 nm for both the parallel and the antiparallel isomer.[22] A small but significant increase in this CD band upon addition of Tre was observed for the parallel isomer of TyrTyr (Figure 4a), thus indicating that the conformation of the disulfide bonds of the cyclic peptide changes upon binding of the carbohydrate. The CD effect was plotted in a Job plot, which has a pronounced maximum at 0.5, thus indicating a 1:1 stoichiometry of the complex (Figure 4b). Indeed, the CD data could be readily fitted with a 1:1 model to give a binding constant $K_a = 802\ M^{-1}$ that corresponds to a free energy of binding $\Delta G = -16.7\ kJ\,mol^{-1}$ (Figure 4c). These findings are entirely consistent with the ITC data reported in Table 1. In the case of the antiparallel isomer of TyrTyr, a small yet significant decrease in the CD signal at 230 nm[22] occurred upon addition of Tre (Figure 5a). The data from this titration could also be readily fitted to a 1:1 model (Figure 5b), thus giving a slightly higher binding constant $K_a = 1.21 \times 10^3\ M^{-1}$ that corresponds to a free energy of binding $\Delta G = -17.7\ kJ\,mol^{-1}$, which again is in good agreement with the data obtained from ITC titrations. Thus, CD measurements indicate that parallel and antiparallel TyrTyr receptors have different conformations, which each undergo a significant rearrangement upon binding of the carbohydrate Tre.

Quantum chemical calculations

Quantum chemical calculations were performed for the complexes of the parallel isomer of HisHis with NANA and MeGal. For the sake of comparison, calculations were also performed for the nonbinding combinations of the parallel isomer of HisHis with MeMan as well as the antiparallel isomer of HisHis with MeGal. Furthermore, the complexes of the parallel and antiparallel complexes of TyrTyr with Tre were calculated. It is reasonable to assume that the carboxylic acid group of NANA is deprotonated at neutral pH ($NANA^{-1}$). The pK_a values of the amino acids ($pK_{a,COOH}$ Cys = 1.7 and pK_{a,NH_2} Cys = 10.4) suggest that the peptides should exist in a zwitterionic form at neutral

pH in an aqueous environment. However, the neutral form is more stable in the gas phase owing to the lack of solvation,[23,24] and therefore the density functional geometry optimizations were performed on the neutral form of the peptides. To test the effect of the protonation state in the gas phase, we calculated the mono-, di-, and triprotonated HisHis binding energies with $NANA^{-1}$, which resulted in values of −202, −405, and −685 kJ mol^{-1}, respectively, at the BLYP-D3/def2-TZVP level of theory. This is to be expected as the Coulombic interaction increases in the absence of the solvent environment. To investigate the effect of an implicit solvation model, conductor-like screening model (COSMO)-corrected ($\varepsilon = 78.25$) binding energies of all complexes are reported in Table 2. A set of diverse starting orientations were created for each combination of peptide and carbohydrate. We optimized 64 separate conformations for each complex, and we observed a large variety of binding energies (see the Supporting Information). The average binding energies of the three lowest-energy conformations (BLYP-D3/def2-TZVP) are tabulated in Table 2.

Table 2. Average electronic binding energy (BE) of the three lowest conformations at the BLYP-D3/def2-TZVP level of theory.[a]

Complex	BE^{gas} [kJ mol^{-1}]	BE^{COSMO} [kJ mol^{-1}][a]
paraHisHis@$NANA^{-1}$	−202.1	−47.81
paraHisHis@$(NANA^{-1})_2$	−211.2	−87.27
paraHisHis@MeGal	−60.02	−24.87
paraHisHis@MeMan	−36.33	−8.99
antiHisHis@MeGal	−28.97	+6.79
paraTyrTyr@Tre	−102.8	−33.50
antiTyrTyr@Tre	−111.3	−37.81

[a] Solvent binding energies were obtained using COSMO $\varepsilon = 78.25$.

Carbohydrate complexes of HisHis

The parallel and antiparallel isomers of HisHis were each optimized in the gas phase by using DFT. The parallel and the antiparallel alignment of the tripeptides in the macrocycle lead to very different conformations. The gas-phase conformation of the parallel isomer of HisHis is best described as an "open" form, whereas the conformation of the antiparallel isomer appears much more compact and resembles a helical motif (see Figure 6). The antiparallel isomer of HisHis was calculated to be around 10 kJ mol^{-1} more stable than the parallel isomer in the gas phase in the absence of any carbohydrate. The antiparallel isomer is possibly stabilized owing to the favorable dipole–dipole interaction of the two constituting tripeptides, which are essentially oriented in an antiparallel orientation. These initial findings suggest that the open conformation of parallel HisHis offers easy access to the imidazole moieties and therefore to strong interaction in the case of NANA. In contrast, the compact and helical form of the antiparallel HisHis might hinder carbohydrate binding.

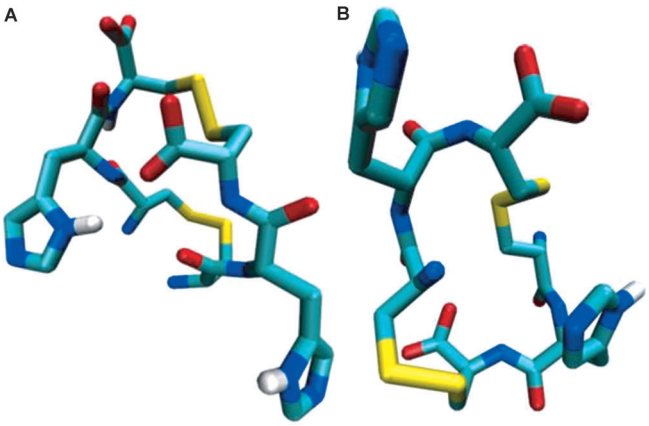

Figure 6. A) Parallel HisHis and B) antiparallel HisHis optimized at the BLYP-D3/def2-TZVP level of theory. Only the hydrogen atoms on the imidazoles are shown. All others are removed to increase the clarity of the diagram.

The 1:1 complex of parallel HisHis with NANA

A preliminary geometry optimization resulted in a lower-energy conformation of the parallel isomer of HisHis bound to NANA in a hypothetical 1:1 complex versus the antiparallel isomer of HisHis bound to NANA in a 1:1 complex. The energy difference was around 20 kJ mol^{-1} at the PM3 level of theory, and the coordinates are provided in the Supporting Information. The preference for the complex with the parallel isomer was also observed in the experimental data. Therefore, we predominately concentrate on the parallel isomer hereafter.

Among the best three gas-phase DFT-optimized structures calculated, the one that shows the highest accordance with the ^{1}H NMR spectroscopic results was selected (Figure 7). This structure shows linear hydrogen bonds (O-H-O angle 176°) of the carboxylate at the C terminus of the peptide with the carboxylic acid and a hydroxyl of NANA. In addition, the structure features a hydrogen bond between the two opposing imidazole rings (N-H-N angle 171°), whereas the second NH is clearly oriented towards the NANA, which suggests another potential hydrogen bond. Thus, the calculated structure shows that NANA binds on the outside of the peptide (*exo* receptor) rather than forming an inclusion complex (*endo* receptor), as

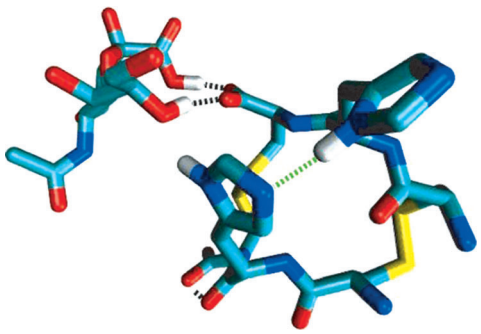

Figure 7. Parallel HisHis bound to NANA (paraHisHis@$NANA^{-1}$) optimized at the BLYP-D3/def2-TZVP level of theory correlating best to the data from ^{1}H NMR spectra. Hydrogen atoms that participate in hydrogen bonding are shown. All others are removed to increase the clarity of the diagram.

might be intuitively expected from a cyclic peptide. The structure also shows that parallel HisHis undergoes a substantial conformational change to optimize hydrogen bonding with NANA, and the interaction involves multiple hydrogen bonds with the peptide backbone as well as the imidazole residues. We emphasize that in the NMR spectra of a 1:1 mixture of parallel HisHis and NANA a pronounced downfield shift of the imidazole protons was observed (see above). Thus, the calculations provide a reasonable explanation for the shifts in the NMR spectroscopic titration. The paraHisHis@NANA^{-1} complex was further modeled in an aqueous medium, that is, an implicit COSMO-type solvation model was used. As can be seen from Table 2, a significant reduction in the binding energy is observed in solution relative to the gas phase. This reduction is to be expected as the charges are effectively screened by the aqueous environment.

The 1:2 complex of parallel HisHis with NANA

In the complex of the parallel isomer of HisHis bound to two molecules of NANA (paraHisHis@(NANA^{-1})$_2$), two possible binding processes were investigated with DFT. A stepwise-like pathway was compared to a concerted case. In the stepwise case, the first NANA initially binds to HisHis, and then a subsequent binding of the second NANA molecule completes the 1:2 complex by using a two-step geometry optimization procedure. Concerted addition occurs when the two NANA molecules simultaneously bind with the HisHis as a 1:2 complex therefore using a one-step geometry optimization procedure. The corresponding binding energies of the 1:2 paraHisHis@(NANA^{-1})$_2$ stepwise complex are given in the Supporting Information, and the best conformation is presented in Figure 8. The optimization procedures failed to converge for the concerted pathway, thus suggesting that the simultaneous binding of two anionic ligands to the HisHis is not energetically favorable. The fact that the stepwise pathway is more favorable in the computations is in accord with the ITC data, which clearly indicate a cooperative binding of NANA.

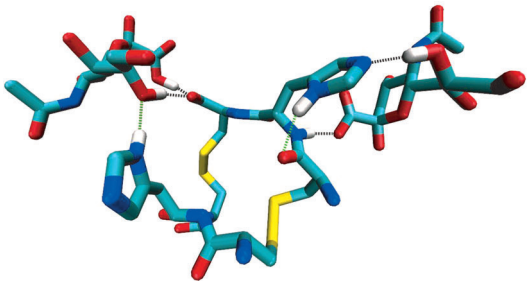

Figure 8. Parallel HisHis bound to two molecules of NANA (para@(NANA^{-1})$_2$) optimized at the BLYP-D3/def2-TZVP level of theory correlating best to the data from ^{1}H NMR spectra. Hydrogen atoms that participate in hydrogen bonding are shown. All others are removed to increase the clarity of the diagram.

Also in this case, the parallel isomer of HisHis acts as an *exo* receptor because both NANA molecules appear to be bound on the outside of the cyclic peptide. Upon comparison of the structures of paraHisHis@NANA^{-1} and paraHisHis@(NANA^{-1})$_2$ it is evident that the peptide unfolds upon binding the second molecule of NANA and that each imidazole ring is now forming hydrogen bonds (O-H-N angle 173 and 172°, and N-H-O angle 177°) with NANA. Furthermore, NANA is also bound by an amide proton in the backbone by a hydrogen bond (N-H-O angle 178°). We note that the hydrogen bonds in the calculated structures correlate with the shifts observed in the ^{1}H NMR spectra (see above). The smaller shift of the imidazole protons upon addition of the second equivalent of NANA relative to the addition of the first one is due to the imidazole ring that serves simultaneously as a hydrogen-bond acceptor and donor. This rearrangement might also explain the large entropy change detected on the second binding event with ITC because water molecules are expelled to the bulk solvent during the second binding of the NANA.

Interestingly, the gas-phase binding energy of the 1:2 complex (−211 kJ mol^{-1}) is only marginally higher than calculated for the 1:1 complex (−202 kJ mol^{-1}), see Table 2, which indicates anticooperative binding in the gas phase. This suggests that solvation plays a substantial role in these receptors, as cooperative binding was observed for the ITC measurements in an aqueous environment. Indeed, the COSMO implicit solvation model calculations show additivity (but not cooperativity) in the 1:2 complex, with approximately twofold binding energy for the 1:2 complex relative to the 1:1 complex (see Table 2).

The 1:1 complexes of parallel and antiparallel HisHis with MeGal

Interestingly, only the parallel isomer of HisHis binds to MeGal with a binding constant that is on the same order of magnitude as for NANA (Table 1). In Figure 9, the gas-phase DFT-optimized structure for the complex paraHisHis@MeGal is shown. The binding energy of this complex in the gas phase is −60 kJ mol^{-1}. It is evident from Figures 7–9 that the structures of the complexes of MeGal and NANA with parallel HisHis show a totally different binding mode. The parallel HisHis *exo*

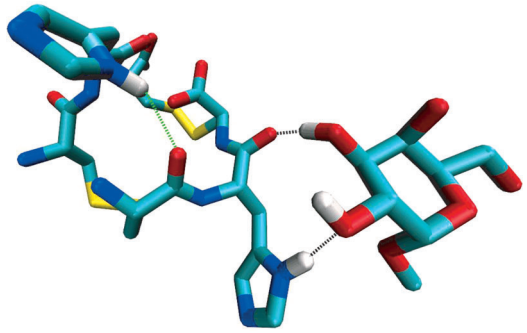

Figure 9. Parallel HisHis bound to MeGal at the BLYP-D3/def2-TZVP level of theory correlating best with data from the ^{1}H NMR spectra. Hydrogen atoms that participate in hydrogen bonding are shown. All others are removed to increase the clarity of the diagram.

receptor binds MeGal through a strong hydrogen bond with the imidazole moieties and the peptide backbone. One of the imidazole moieties forms a hydrogen bond (N-H-O angle 177°) with the MeGal, whereas the second one forms an additional hydrogen bond (N-H-O angle 171°) with the backbone of the peptide (Figure 9). This might be the reason for the observed downfield shift in the ^{1}H NMR spectra for the imidazole protons (Figure 3). On the other hand, protons from Gal show a upfield shift, which indicates a (His)N-H-O(MeGal) interaction because the environment around the aromatic protons is more electron rich in the complex. The reason for the upfield shift of the CH protons of Gal upon binding to parallel HisHis might also be explained by the formation of hydrogen bonds (N-H-O angle 178°) between the receptor and the OH function on C2 and C3 of the carbohydrate. A significant binding energy of -24.9 kJ mol^{-1} is also observed when using a solvation model for the complex between parallel HisHis and MeGal (Table 2). This binding energy is substantially lower than for the complexes of HisHis with NANA (see Table 2). This reduction in binding energy is presumably related to the absence of formal charge on MeGal so that it may be assumed that electrostatic interactions significantly stabilize the gas-phase complex of parallel HisHis and NANA.

In contrast, although a weak binding is observed in the gas-phase calculation for the complex of antiparallel HisHis and MeGal (see Figure S11 in the Supporting Information), no binding is found when a solvation model is employed (Table 2). To verify whether the selectivity observed by experiment is reproduced by the DFT calculations, another negative control calculation was carried out: the hypothetical complex of parallel HisHis and MeMan was also calculated (see Figure S12 in the Supporting Information). Although significant interaction is calculated for the gas phase, only a very small binding energy (-9 kJ mol^{-1}) is observed when using a solvation model. Thus, the results from the calculations are entirely consistent with the experimental data.

Carbohydrate complexes of TyrTyr

The relative stabilities of the parallel and antiparallel isomers of TyrTyr in the gas phase were computed with DFT calculations (see Figure 10). The antiparallel isomer was found to be around 13 kJ mol^{-1} more stable than the parallel isomer. This is presumably owing to the intramolecular hydrogen bonding of the peptide backbones in the antiparallel isomer. The gas-phase DFT-optimized structure of the parallel isomer displays no such intramolecular hydrogen-bonding interaction. In addition, the antiparallel isomer is possibly stabilized owing to the favorable dipole–dipole interaction of the constituting tripeptides, which are essentially oriented in an antiparallel orientation (as described above for HisHis). Also in this case, the parallel isomer appears to have a rather "open" conformation, whereas the antiparallel is more compact and "closed". We note that the differing conformations of the parallel and antiparallel isomers are also clearly observed in the CD spectra (see Figures 4 and 5)

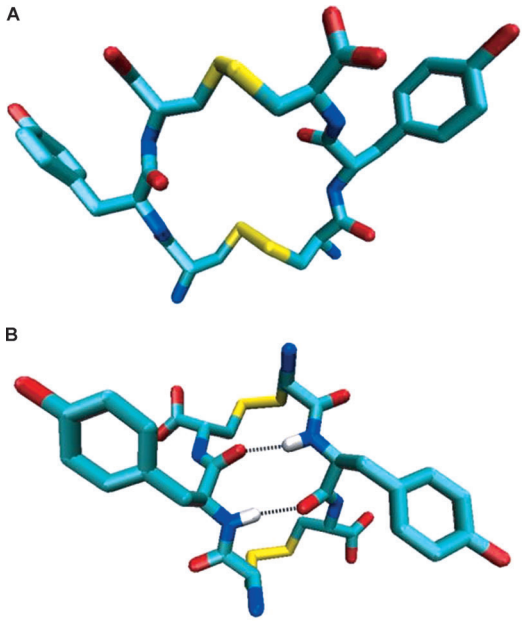

Figure 10. A) Parallel TyrTyr and B) antiparallel TyrTyr at the BLYP-D3/def2-TZVP level of theory. Hydrogen atoms that participate in hydrogen bonding are shown. All others are removed to increase the clarity of the diagram.

The 1:1 complexes of parallel and antiparallel TyrTyr with Tre

In contrast to the parallel and antiparallel HisHis receptors described above, the parallel and antiparallel TyrTyr show nearly identical binding constants for the interaction with Tre in the ITC and CD experiments. The DFT-optimized paraTyrTyr@Tre and antiTyrTyr@Tre complexes are presented in Figure 11. It can be observed that the structure of paraTyrTyr@Tre exhibits hydrogen bonding to the carboxylate terminus of the peptide to form a rather "open" complex. Tre is bound by two hydrogen bonds (O-H-O angle 177°) to the C=O and N–H functions of two adjacent amide bonds of parallel TyrTyr. Furthermore, a nonlinear hydrogen bond (O-H-O angle 168°) is formed between the carboxylate terminus of the receptor and an OH function of Tre. Thus, the complex features three strong hydrogen bonds between the peptide and the carbohydrate, and the cyclic peptide appears to function as an *exo* receptor. In contrast, the antiTyrTyr@Tre complex features a hydrogen-bond interaction of the OH at the C6 of Tre with the Tyr side group (O-H-O angle 178°) and moreover additional hydrogen bonds (O-H-O angle 171°) between the C and N terminus of the backbone and the OH at C3 and C4 of Tre. Thus, the calculations suggest that Tre is bound exclusively through hydrogen bonding with the peptide backbone of parallel TyrTyr, whereas it forms hydrogen bonds with the tyrosine moiety as well as the peptide backbone of antiparallel TyrTyr. Finally, the optimized complexes paraTyrTyr@Tre and antiTyrTyr@Tre suggest that Tre binds slightly more strongly to the antiparallel isomer than to the corresponding parallel isomer of TyrTyr. This difference at the DFT level of theory in the gas phase is around 10 kJ mol^{-1} and reduces to around 4 kJ mol^{-1} with the inclusion of solvation in the COSMO model. This small energetic difference between the isomers is at least qualitatively in accord

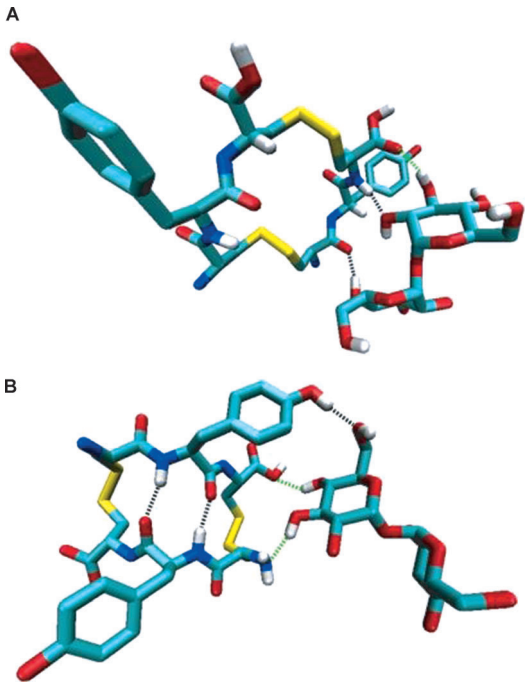

Figure 11. Complexes of A) parallel and B) antiparallel TyrTyr with trehalose at the BLYP-D3/def2-TZVP level of theory. Structures that correlate best with the data from the ^{1}H NMR spectra are shown. Hydrogen atoms that participate in hydrogen bonding are shown. All others are removed to increase the clarity of the diagram.

with our reported ITC and CD data, which shows very similar binding constants for both isomers of TyrTyr with Tre.

Conclusion

We have investigated two biomimetic carbohydrate receptors, HisHis and TyrTyr, which are composed of two tripeptides, Cys-His-Cys and Cys-Tyr-Cys, linked by two disulfides. The parallel and antiparallel isomer of each cyclic peptide was synthesized separately. It was found that the parallel isomer of HisHis binds NANA with a significantly higher affinity than the corresponding antiparallel isomer. Nevertheless, both isomers are high-affinity receptors for NANA, and they display a cooperative binding of two molecules of NANA in aqueous solution at neutral pH. In contrast, although the parallel HisHis isomer binds strongly to MeGal, no interaction was found for the antiparallel HisHis and MeGal by ITC and NMR spectroscopy. In the case of the TyrTyr isomers and Tre, the antiparallel isomer has a slightly higher affinity towards the carbohydrate target than the parallel isomer. Four other very similar carbohydrates showed no significant interaction with any isomer of the two peptides. Quantum chemical calculations were used to model these peptide–carbohydrate complexes. With reference to ^{1}H NMR spectroscopy water suppression experiments, a possible complex structure was selected from the three best DFT structures. Furthermore, the inclusion of implicit solvation models was found to be crucial to understand the relative difference between the complexes in experiments. Differences in the affinities for each carbohydrate may be explained by the totally different conformations of the each isomer. Whereas the parallel isomer of HisHis has an open structure by which the imidazole moieties can be easily accessed, the antiparallel isomer of HisHis has a closed structure that might hamper the interaction between the imidazoles and the carbohydrate. According to the calculations, both HisHis and TyrTyr are *exo* receptors for their carbohydrate targets, which are not included in the macrocycle but bind edge-on to the peptides. The calculations confirm the selectivity observed in the experiments and indicate the formation of multiple intermolecular hydrogen bonds in the most stable complexes. These findings have significantly increased our understanding of a new class of biomimetic carbohydrate receptors that had previously been identified using a dynamic combinatorial library of peptides. It is hoped that one day these receptors may find application in biomedicine and biotechnology.

Experimental Section

HPLC

The parallel and antiparallel isomers as well as the mixture of isomers were analyzed with a LC setup that comprised a Shimadzu LC20 prominence HPLC system. For controlling the LC, LCsolutions (version 1.0.0.1, Shimadzu) was used. The separation was carried out using a ZORBAX HILIC Plus, 2.1×100 mm, 3.5 μm. The flow rate was 0.10 mL min^{-1}, the oven was maintained at 25 °C, and the injection volume was 5 μL. Acetonitrile (90%) and NH_4OAc (10%, 10 mM, pH 6.8) were used as the mobile phase. The complete run time was set to 55 min. Samples were prepared by dissolving a minimum amount of the solid peptide in 1 mL ACN/NH_4OAc (90:10).

Isothermal titration calorimetry

ITC measurements were performed using a NanoITC system (Calorimetry Sciences Cooperation, USA) and ITC Run software. Sample solutions were prepared by dissolving the appropriate amount of peptide in phosphate buffer (100 mM, pH 7.4). Before filling the cell, the solution was degassed for 30 min. The peptide—2 mM for parallel HisHis and TyrTyr, or 1 mM for antiparallel HisHis and TyrTyr—was titrated with a degassed solution (30 min) of NANA (40 mM), MeGal (25 mM), or Tre (12 mM) in phosphate buffer. All measurements were performed at 23 °C using a stirring rate of 300 rpm and a 400 s interval between each injection. To determine the heat of dilution, a carbohydrate solution was titrated into phosphate buffer (100 mM, pH 7.4). The heat of dilution was subtracted from the raw heat data. The data was fitted to a 1:1 or 1:2 model by using a spreadsheet method.[25]

^{1}H NMR spectroscopic water suppression experiments

The NMR spectroscopic samples were prepared by dissolving the appropriate amount of peptide and carbohydrate in phosphate buffer (0.8 mL, 100 mM, pH 7.4). Typically, peptide (2 mM) was mixed with carbohydrate (0, 2, 4, or 10 mM). After mixing, the samples were measured using a Varian Inova 500 NMR at 300 K using the 1D wet sequence to suppress the water signal. Chemical shifts are reported as relative values versus tetramethylsilane and were calculated using MestReNova (version 6.0.3–5604, MestRelab Research S.L.).

CD titrations

CD titrations were performed using a J815 CD spectrometer (JASCO). The data were analyzed using OriginPro 8.0 (OrginLab Cooperation, Northhampton, USA, version 8.0724(B724)). As background, the used phosphate buffer was measured and subtracted after measuring each sample. A 1.0 mM solution of parallel TyrTyr or a 2.0 mM solution of antiparallel TyrTyr in phosphate buffer was put into a quartz glass cuvette (104F-QS, 10.00 mm, Brand), measured from 180 to 300 nm nine times, and afterwards accumulated using the Spectra Manager Version 2 software (version 2.08.04, JASCO). An 80 mM Tre solution in buffer was added in 1.7 μL steps. A blank measurement was performed by titrating the corresponding aliquots of buffer into a 1.0 or 2.0 mM peptide solution. All measurements were performed after mixing the solutions and waiting for 60 s before starting the measurements. The data were fitted to a 1:1 model.

Computational methods

Herein we applied a multi-tiered meta-optimization strategy:

1) The metaheuristic particle swarm optimization (PSO) technique was employed to iteratively improve on a candidate solution with regards to maximizing the binding energy. The particle swarm optimization calculations were carried out using an in-house code that utilizes the JSwarm API.[26] The dimensions of acceptable search space were determined by trial and error. In total twelve degrees of freedom were used as the search space (x, y, z, α, β, γ), which are simply a Cartesian framework with corresponding Euler angles for rigid rotation. The internal degrees of freedom for the monomers were frozen.

2) A simulated annealing (SA)-based approach was used, whereby a single carbohydrate molecule binds to the HisHis (1:1) or a dimer (1:2) is constructed in either a concerted or stepwise fashion. Ten diverse structures were heated to 600 K, simulated for 300 ps, then cooled to 300 K, and simulated for a further 300 ps. The atom-centered density matrix propagation (ADMP) method implemented within Gaussian 09[27] was used for the molecular dynamics trajectories. The PM3 Hamiltonian was used for the ADMP trajectories. A total of ten high/low cycles were performed, and a single random snapshot was extracted from each of the cooling cycles, therefore we generated 640 conformations for each complex. We have randomly taken 64 conformers to be subsequently optimized with DFT in the subsequent step.

3) For the DFT calculations, TURBOMOLE was used with the BLYP functional combined with Grimme's third-generation dispersion correction, in conjunction with the def2-TZVP[28] basis set. The resolution-of-the-identity approximations together with suitable auxiliary fitting functions from the TURBOMOLE library were applied throughout. The corresponding binding energies are shown in the above (see Table 2).

4) COSMO was invoked within TURBOMOLE 6.3[29] to model solvation effects. COSMO is a well-known continuum solvation model, whereby a cavity within a dielectric continuum of permittivity (ε) is created by the solute molecule. The dielectric constant of $\varepsilon = 78.35$ was chosen to model the aqueous environment of the experiment. COSMO single-point energies were computed at the RI-BLYP/def2-TZVP level of theory (see Table 2).

Acknowledgements

The Deutsche Forschungsgemeinschaft (DFG) is gratefully acknowledged for financial support (IRTG 1143 and SFB 858). This work was supported by COST CM1005 "Supramolecular Chemistry in Water".

Keywords: carbohydrates · lectins · molecular recognition · peptides · receptors

[1] H. Lis, N. Sharon, *Chem. Rev.* **1998**, *98*, 637 – 674.
[2] a) A. Varki, *Glycobiology* **1993**, *3*, 97 – 130; b) R. A. Laine, *Glycobiology* **1994**, *4*, 759 – 767; c) B. T. Houseman, M. Mrksich, *Top. Curr. Chem.* **2002**, *218*, 1 – 44; d) T. K. Lindhorst, *Essentials of Carbohydrate Chemistry and Biochemistry*; Wiley-VCH Weinheim, **2007**.
[3] a) A. P. Davis, R. S. Wareham, *Angew. Chem.* **1999**, *111*, 3160 – 3179; *Angew. Chem. Int. Ed.* **1999**, *38*, 2978 – 2996; b) S. Kubik, *Angew. Chem.* **2009**, *121*, 1750 – 1753; *Angew. Chem. Int. Ed.* **2009**, *48*, 1722 – 1725.
[4] a) E. Klein, M. P. Crump, A. P. Davis, *Angew. Chem.* **2005**, *117*, 302 – 306; *Angew. Chem. Int. Ed.* **2005**, *44*, 298 – 302; b) Y. Ferrand, M. P. Crump, A. P. Davis, *Science* **2007**, *318*, 619 – 622; c) K. Ramírez-Gualito, R. Alonso-Rios, B. Quiroz-Garcia, A. Rojas-Aguilar, D. Diaz, J. Jimenez-Barbero, G. Cuevas, *J. Am. Chem. Soc.* **2009**, *131*, 18119 – 18128; d) M. Mazik, *Chem. Soc. Rev.* **2009**, *38*, 935 – 956; e) Y. Ferrand, E. Klein, N. P. Barwell, M. P. Crump, J. Jiménez-Barbero, C. Vicent, G.-J. Boons, S. Ingale, A. P. Davis, *Angew. Chem.* **2009**, *121*, 1807 – 1811; *Angew. Chem. Int. Ed.* **2009**, *48*, 1775 – 1779; f) N. P. Barwell, M. P. Crump, A. P. Davis, *Angew. Chem.* **2009**, *121*, 7809 – 7812; *Angew. Chem. Int. Ed.* **2009**, *48*, 7673 – 7676; g) N. P. Barwell, A. P. Davis, *J. Org. Chem.* **2011**, *76*, 6548 – 6857.
[5] a) G. Wulff, *Angew. Chem.* **1995**, *107*, 1958 – 1979; *Angew. Chem. Int. Ed. Engl.* **1995**, *34*, 1812 – 1832; b) S. Striegler, *Curr. Org. Chem.* **2003**, *7*, 81 – 102; c) G. Heinrichs, M. Schellentrager, S. Kubik, *Eur. J. Org. Chem.* **2006**, 4177 – 4186; d) A. Pal, M. Bérubé, D. Hall, *Angew. Chem.* **2010**, *122*, 1534 – 1537; *Angew. Chem. Int. Ed.* **2010**, *49*, 1492 – 1495.
[6] M. Mazik, C. Gefferet, *Org. Biomol. Chem.* **2011**, *9*, 2319 – 2326.
[7] H. Abe, Y. Chida, H. Kurokawa, M. Inouye, *J. Org. Chem.* **2011**, *76*, 3366 – 3371.
[8] C. Ke, H. Destecroix, M. P. Crump, A. P. Davis, *Nat. Chem.* **2012**, *4*, 718 – 723.
[9] M. Rauschenberg, S. Bomke, U. Karst, B. J. Ravoo, *Angew. Chem.* **2010**, *122*, 7498 – 7503; *Angew. Chem. Int. Ed.* **2010**, *49*, 7340 – 7345.
[10] M. P. Waller, H. Kruse, C. Mück-Lichtenfeld, S. Grimme, *Chem. Soc. Rev.* **2012**, *41*, 3119 – 3128.
[11] P. Hobza, J. Sponer, T. Reschel, *J. Comput. Chem.* **1995**, *16*, 1315 – 1325.
[12] J. Černy, P. Hobza, *Phys. Chem. Chem. Phys.* **2005**, *7*, 1624 – 1626.
[13] E. R. Johnson, R. A. Wolkow, G. A. DiLabio, *Chem. Phys. Lett.* **2004**, *394*, 334 – 338.
[14] a) S. Grimme, *J. Chem. Phys.* **2006**, *124*, 034108; b) S. Grimme, J. Antony, S. Ehrlich, H. Krieg, *J. Chem. Phys.* **2010**, *132*, 154104.
[15] P. Jurečka, J. Sponer, J. Cerny, P. Hobza, *Phys. Chem. Chem. Phys.* **2006**, *8*, 1985 – 1993.
[16] L. Gráfová, M. Pitoňák, J. Řezáč, P. Hobza, *J. Chem. Theory Comput.* **2010**, *6*, 2365 – 2376.
[17] S. T. Schneebeli, A. D. Bochevarov, R. A. Friesner, *J. Chem. Theory Comput.* **2011**, *7*, 658 – 668.
[18] a) R. Matsueda, S. Higashida, F. Alberico, D. Andreu, *Peptide Res.* **1992**, *5*, 262 – 264; b) A. K. Galande, A. F. Spatola, *Org. Lett.* **2003**, *5*, 3431 – 3434.
[19] S. Zhang, F. Lin, M. A. Hossain, F. Shabanpoor, G. W. Tregear, J. D. Wade, *Int. J. Pept. Res. Ther.* **2008**, *14*, 301 – 305.
[20] a) D. Andreu, F. Alberico, N. A. Sole, M. C. Munson, M. Ferrer, G. Barany in *Methods in Molecular Biology* (Eds: M. W. Pennington, B. M. Dunn), Humana Press: Totowa, **1994**, **pp.** 91 – 160; b) M. S. Bernatowicz, R. Matsueda, G. R. Matsueda, *Int. J. Pept. Protein Res.* **1986**, *28*, 107 – 112; c) A. Schulz, K. Adermann, M. Eulitz, S. M. Feller, C. Kardinal, *Tetrahedron* **2000**, *56*, 3889 – 3891.
[21] a) T. L. Hwang, A. J. Shaka, *J. Magn. Reson. Ser. A* **1995**, *112*, 275 – 279; b) P. Besenius, K. P. van den Hout, H. M. H. G. Albers, T. F. A. de Greef, L. L. C. Olijve, T. M. Hermans, B. F. M. de Waal, P. H. H. Bomans, N. A. J. M.

Sommerdijk, G. Portale, A. R. A. Palmans, M. H. P. van Genderen, J. A. J. M. Vekemans, E. W. Meijer, *Chem. Eur. J.* **2011**, *17*, 5193 – 5203.
[22] G. Pescitelli, L. Di Bari, N. Berova, *Chem. Soc. Rev.* **2011**, *40*, 4603 – 4625.
[23] K. Ösapaz, W. S. Young, D. Bashford, C. L. Brooks, D. A. Case, *J. Phys. Chem.* **1996**, *100*, 2698 – 2705.
[24] M. Knapp-Mohammadya, K. J. Jalkanena, F. Nardib, R. C. Wadeb, S. Suhaia, *Chem. Phys.* **1999**, *240*, 63 – 77.
[25] J. Huskens, H. van Bekkum, J. A. Peters, *Comput. Chem.* **1995**, *19*, 409 – 416.
[26] P. Cingolani, http://jswarm-pso.sourceforge.net/.
[27] Gaussian 09, Revision A.1, M. J. Frisch, G. W. Trucks, H. B. Schlegel, G. E. Scuseria, M. A. Robb, J. R. Cheeseman, G. Scalmani, V. Barone, B. Mennucci, G. A. Petersson, H. Nakatsuji, M. Caricato, X. Li, H. P. Hratchian, A. F. Izmaylov, J. Bloino, G. Zheng, J. L. Sonnenberg, M. Hada, M. Ehara, K. Toyota, R. Fukuda, J. Hasegawa, M. Ishida, T. Nakajima, Y. Honda, O. Kitao, H. Nakai, T. Vreven, J. A. Montgomery, Jr., J. E. Peralta, F. Ogliaro, M. Bearpark, J. J. Heyd, E. Brothers, K. N. Kudin, V. N. Staroverov, R. Kobayashi, J. Normand, K. Raghavachari, A. Rendell, J. C. Burant, S. S. Iyengar, J. Tomasi, M. Cossi, N. Rega, J. M. Millam, M. Klene, J. E. Knox, J. B. Cross, V. Bakken, C. Adamo, J. Jaramillo, R. Gomperts, R. E. Stratmann, O. Yazyev, A. J. Austin, R. Cammi, C. Pomelli, J. W. Ochterski, R. L. Martin, K. Morokuma, V. G. Zakrzewski, G. A. Voth, P. Salvador, J. J. Dannenberg, S. Dapprich, A. D. Daniels, Ö. Farkas, J. B. Foresman, J. V. Ortiz, J. Cioslowski, D. J. Fox, Gaussian, Inc., Wallingford CT, **2009**.
[28] A. Schäfer, C. Huber, R. Ahlrichs, *J. Chem. Phys.* **1994**, *100*, 5829 – 5835.
[29] TURBOMOLE V6.3 2011, a development of University of Karlsruhe and Forschungszentrum Karlsruhe GmbH, 1989 – 2007, TURBOMOLE GmbH, since 2007; available from http://www.turbomole.com.

Received: September 26, 2013
Published online on February 13, 2014